IPAC REPORT

A USER'S GUIDE TO IRAS POINTED OBSERVATION PRODUCTS

E. T. Young, G. Neugebauer, E. L. Kopan, T. D. Benson,
T. P. Conrow, W. L. Rice, D. T. Gregorich

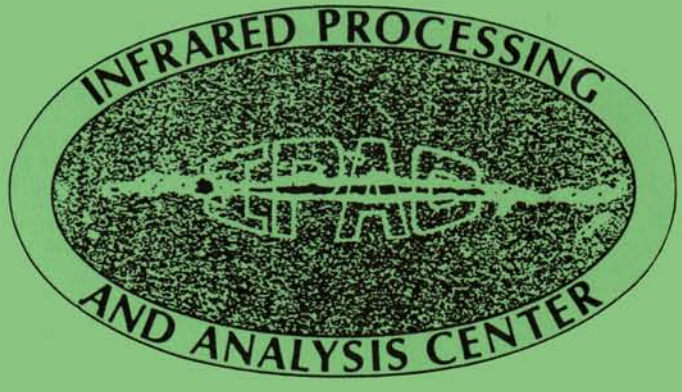

A USER'S GUIDE TO IRAS POINTED OBSERVATION PRODUCTS[1]

E.T. YOUNG

G. NEUGEBAUER

E.L. KOPAN

R.D. BENSON

T.P. CONROW

W.L. RICE

D.T. GREGORICH

[1] To be distributed by the National Space Science Data Center, Greenbelt, Maryland, and through Infrared Processing and Analysis Center, Pasadena, California

The Infrared Astronomical Satellite was developed and is operated by the Netherlands Agency for Aerospace Programs (NIVR), the US National Aeronautics and Space Administration (NASA), and the UK Science and Engineering Research Council (SERC).

1985 November 29

INDEX

TABLES

I. INTRODUCTION

During the ten month lifetime of the Infrared Astronomical Satellite (IRAS), roughly 40% of the observing time was devoted to pointed observations of selected objects. Nearly ten thousand of these observations, also commonly called Additional Observations (AO's) were made of virtually every kind of astronomical object using either the survey array or the Chopped Photometric Channel (CPC). Observations made with the CPC were processed in the Netherlands, while those made with the survey array were processed at the Infrared Processing and Analysis Center (IPAC), an outgrowth of the Science Data Analysis System (SDAS) at the Jet Propulsion Laboratory (JPL).

This guide covers the use of the standard data products from IPAC. Many details of the IRAS mission, satellite, data reduction and calibration are given in the Explanatory Supplement to the IRAS Catalog and Atlases (1985), henceforth known as The Supplement). An acquaintance with the cautions listed therein is essential.

This guide is intended both for users familiar with the data products as well as new users. The guide is a major revision of the AO Interpreter edited by George Miley. Substantial improvements in the quality of the products have been made since the time that guide was written.

II. THE OBSERVATIONS

Pointed observations were made using very well defined command sequences or macros stored in the satellite's computer. The macros are designated by a three letter name indicating the general class of the macro, a 2 digit number identifying the specific type and a single letter indicating the version. The different macro types are listed in Table 1, while the characteristics of the macros actually used in practice are given in Table 2.

Although the number of specific different macros is large, the vast majority of the survey array observations were made with only a few of these macros. The DPS macros are by far the most important numerically. In these macros, the satellite scanned an area of sky a number of times using the entire survey array, producing infrared maps of the observed region. Scan lengths ranged from 1.6 degrees to 6 degrees. Other possible variations, each given a different number in the macro name, included the number of scan legs and the size of the cross-scan step between scan legs.

The DPP, DMS and DNS macros were the next most commonly used macros especially in the beginning of the mission. The targeted source was repeatedly scanned over a selected detector in each band. Roughly midway through the mission, the use of the DPP macros was discontinued in favor of the DPS varieties because of the greater sky coverage available with the latter, because it was difficult to determine the real

background levels with the DPP macro and because there was no advantage in the signal to noise ratio obtained with the DPP macros over that obtained with comparable observing time DPS macros. Primarily due to difficulties in verifying the quality of the DPP, DMS, and DNS observations, they are not being included in the present release of the AOs. We anticipate that with additional analysis and processing a product suitable for general distribution will forthcoming in the near future.

The DSD macro was a special mapping procedure that used only the small edge detectors of the focal plane array to produce a map with high angular resolution. A box of roughly 10' x 10' was fully covered in the four bands.

Table 1. Macro Characteristics

Macro	Type of Observation
DPS	Deep Field: Half-survey rate raster scans
DPM	Mapping: Survey rate raster scans with specifiable cross scan step
SLM	Monitor: Survey-like scans mainly to get low resolution spectra of bright sources
DSD	High Resolution: Mapping in four bands using small edge detectors
DPP	Photometry: Short rasters over best detector in each band default detectors:21,23,37,6 except DPP55D which uses 53,44,14,6
DMS	Deep scan: 10' scans across center of specified detector default detectors: 53,44,14,6
DNS	Long scan: 20' scans across center of specified detector default detectors: 23,21,37,6

Macros discontinued after in-flight tests

DPB	Beam Switch: Five alternating dwells on two detectors at 60 and 100 um
DPC	Chopping: Detector pointed to position 1 for a dwell time dt, slewed to position 2 for a dwell time dt
DBM	Burst Monitor: Two stares for 60s each with specified 60 and 100 um detectors
DQB	Quick Monitor: 30 sec stares with specified 60 and 100 um detectors

Table 2. Macro Characteristics

Macro Name	Number Scans	Bands	Scan length (')	Cross step (')	N FAC+	Obs time (s)	Speed++	SNR gain
DPS02B	6	all	96	0.3	2	428	1/2	4.8
DPS05B	3	all	360	1.0	2	644	1/2	3.5
DPS52B	6	all	96	0	2	428	1/2	4.8
DPS55B	3	all	360	0	2	644	1/2	3.5
DPS60B	4	all	60	0.8	2	244	1/2	4.0
DPS60D	5	all	48		1	249	1/2	4.4
DPS61C	12	all	60	0.17	1	596	1/2	6.9
DPS61D	14	all	48	0.2 **	1	634	1/2	7.7
DPS62D	9	all	96	0.4	1	583	1/2	6.0
DPS63D	3	all	96	0.8	1	254	1/2	3.5
DPM06B	6	all	180	<28	2	443	1	1.4-3.2
DPM06D	7	all	180	<28	1		1	1.4-4.0
SLM15B	4	all	60	<28	2	257	1	1.0
SLM16B	8	all	120	<28	2	627	1	1.0
SLM17B	6	all	72	<28	2	389	1	1.0
SLM17D	6	all	72	<28	1	390	1	1.0
DSD01A	18	all	28	0.5	2	464	1/2	
DPP08C	16	12,25		0.2	2	447	1/4	8.0*
DPP13C	12	60,100		0.3	2	449	1/4	6.9*
DPP43C	7	all		0.5	2	437	1/4	5.3*
DPP44C	10	all		0.3	2	605	1/4	6.3*
DPP51C	14	12,25		0.2	2	457	1/8	10.6*
DPP52C	9	60,100		0.2	2	461	1/8	8.5*
DPP53C	6	all		0.5	2	477	1/8	6.9*
DPP54C	8	all		0.4	2	621	1/8	8.0*
DPP55C	7	12,25		0.5	2	265	1/8	7.5*
DPP55D	6	all		0	2	592	1/8	6.9*
DMS01B	9	all		0	2	649	1/2	4.2
DMS02B	17	60,100		0	2	639	1/2	5.8
DMS03B	17	12,25		0	2	639	1/2	5.8
DMS11B	5	all		0	2	645	1/8	4.0*
DMS12B	9	60,100		0	2	605	1/8	6.0*
DMS13B	9	12,25		0	2	605	1/8	6.0*
DNS01A	6	all		0	2	605	1/2	3.5
DNS02A	13	60,100		0	2	628	1/2	5.1
DNS03A	13	12,25		0	2	628	1/2	5.1

++ Speed is in units of survey scan rate. 1 = 3.85'/second.
+ N FAC is the number of fine attitude calibrations.
* Theoretical SNR gain based on dwell time. Not realized due to excess low frequency noise.
** Coarser outside of central area covered

III. SCIENTIFIC PROGRAM

It was agreed from the start that, although the pointed observations should occupy about 40% of the observing time, the all-sky survey would have first priority in the selection of the actual observing targets. As a method of deciding on the targets for the pointed observations, the Joint IRAS Science Working Group (JISWG) divided into seven smaller working groups, each of which selected the targets for an area of scientific interest. The JISWG as a whole decided on relative priorities by allocating a total number of targets each group could assign first and second priority to. Each sub-group then assigned priorities to each of the objects in their potential list of targets. In practice, the complexities of the scheduling and the overall highest priority assigned to the survey, coupled with the limited area in which the telescope could point, meant that pointed observations were not carried out on priority standing alone. Additionally, a large "shopping list" of targets evenly spaced on the sky was available if no higher priority targets were suitable during a given observing period. It sometimes occured that a target with low priority was observed while first priority targets in another region of the sky were not observed.

The sub-groups, and the coordinators of each, were:

sub-group	coordinator
(AG) Active galaxies	G. Neugebauer
(BS) Bright stars	F. Gillett
(CG) Close galaxies	H. Habing
(DF) Deep fields	E. Young
(MC) Molecular clouds	R. Jennings
(GS) Galactic structue	F. Olnon
(SY) Solar system	R. Walker

A typical pointed observation took about 15 minutes. Observing constraints, however, did not always permit targets from the scientific program to be observed. A few months into the mission it was realized that the automatic scheduling program therefore left times when no observations were made. As a result, locations were picked on a relatively uniform grid in ecliptic coordinates where the telescope was pointed whenever one of these gaps potentially occured; the coordinator of this effort (the FL sub-group) was G. Neugebauer. Late in the mission, several objects found in processing the survey were also made into targets for the pointed observations. The coordinator of this effort (the SF sub-group) was F. Low. The originating group for a given observation is identified in the "OBJECT" field of the grid header.

IV. IPAC DATA PRODUCTS

The primary data products of the pointed observations are the "deep sky grids", produced by the Deep Sky Coadding (DSCO) processor. Each DSCO grid consists of eight two-dimensional arrays of numbers (called maps) produced by coadding the observations. The eight maps represent the signal and the noise in each of the four IRAS wavelength bands. A basic assumption used in generating the grids is that the contribution of each detector is weighted inversely as the square of its noise. To maximize the transportablity of these data to the astronomical community, the released grids are distributed in the standard FITS format (Wells, Greisen, and Harten. 1981, Astron. and Astrophys., [Suppl.], 44, 363.) A detailed description of the FITS header can be found in Appendix A.

There are two kinds of grids, FLUX mode and INTENSITY or INTN mode grids. For the FLUX grids, the data are filtered with a zero-sum band-pass filter centered on the point source spatial frequency. The extended information is suppressed, but in uncomplicated fields, the highest sensitivity for the detection of point sources is obtained. FLUX grid outputs are in units of Jy.

The important processing steps in producing FLUX grids are:

1. Conversion of the detector data stream into a calibrated collection of samples.

2. Removal of residual radiation hits and other glitches from the data.

3. Bandpass filtering of the detector data.

4. Mapping the detector samples to a spatial grid using the reconstructed pointing data.

5. Binning the data in a two-dimensional spatial grid.

6. Computing the weighted flux estimate.

7. Application of suitable calibration factors.

The detector data stream is deglitched using a simple algorithm that compares the power in a high frequency (or glitch) band to the power in a band centered on the point source frequency. If the glitch is of sufficient amplitude and if the ratio of the power in the glitch band to the power in the source band exceeds a predetermined threshold, three samples are removed from the data stream. This filter sucessfully removes over 90% of the narrow glitches from the data.

The band-pass filter used for the FLUX grids is a rectangular zero-sum filter centered on the point-source frequency. Figures 1 and 2 show the in-scan signature for an unfiltered (or INTN) and filtered (or FLUX)

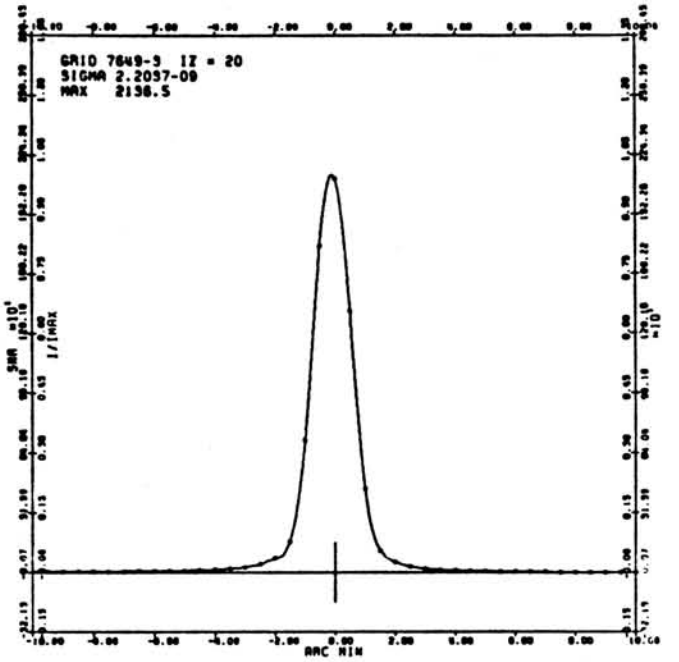

Figure 1. INTENSITY In-Scan Point Source Signature, 60 um Band

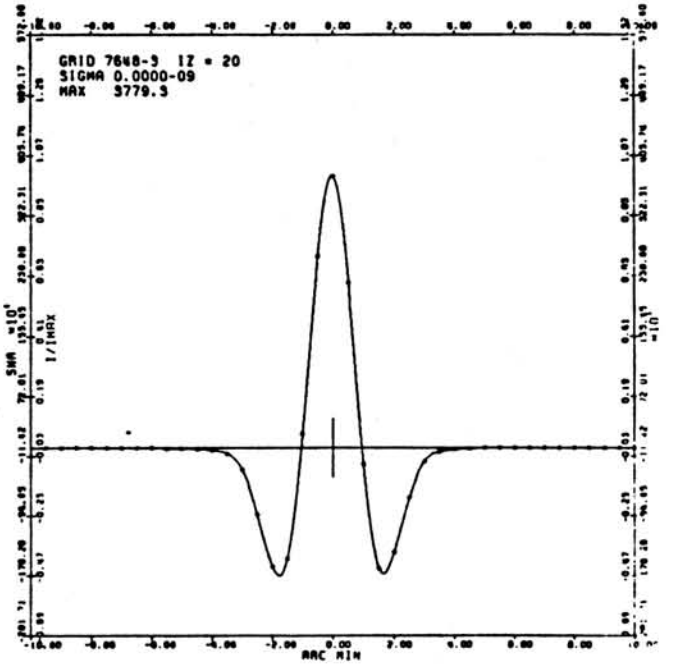

Figure 2. FLUX In-Scan Point Source Signature, 60 um Band

point source, respectively. These plots are for the 60 um band. The FLUX grids are calibrated so that the peak amplitude above the baseline is proportional to the flux density of a point source. Extended sources will have systematically low flux densities on FLUX grids.

The detector data to be combined in a given pixel are weighted for minimum variance using a median noise estimate for each detector. The noise estimator is similar to the one used in producing the Point Source Catalog, which is discussed in Section V.C of the Supplement. If f_i is a flux sample going into a pixel and n_i is the noise estimate associated with each sample, the averaged flux <f> for N samples is given by:

$$\langle f \rangle = \frac{\sum f_i \, w_i}{\sum w_i}$$

where the weighting factor $w_i = (n_i)^{-2}$.

A noise map is provided with the data. The sample variance is combined with the detector noise weights to produce a noise estimate for each pixel. The Chi-Square for a cell is defined as:

$$\chi^2 = \sum f_i^2 \, w_i - (\sum w_i) \langle f \rangle^2$$

The estimated LOCAL noise $< \sigma >$ is then:

$$< \sigma > = \sqrt{\frac{1 + \chi^2}{N \sum w_i}}$$

This LOCAL noise tends to equal the minimum variance estimate for a small number of scans, but approaches the sample variance for a large number of scans. The estimated noise is sensitive to source structure in complex fields (such as molecular clouds), and can be artificially high in such areas.

INTENSITY grids are spatially smoothed but not bandpass filtered, preserving the total intensity information (See, however, cautions in Section V.) In addition, the detector baselines are adjusted as needed for first order de-striping before the data are binned into the two dimensional grid. The INTENSITY grids are thus potentially useful in examining extended structure and for obtaining accurate positions in confused regions. An estimate of the local background level in the area covered by the grid was obtained by calculating the 25th percentile of the signal map intensity values. To produce the band maps, this background estimate has been subtracted from the true sky intensities. The 25th percentile background level is encoded in the nonstandard FITS keywork "BIAS". INTENSITY grid outputs are in units of Jy Sr^{-1}.

The pixel sizes used in the grids for the various classes of observations are listed in Table 3.

Table 3.1 -- Grid Parameters

Macro	In-scan pixel (')				Cross-scan pixel (')
	12 um	25 um	60mu	100 um	
DPS	0.25	0.25	0.5	1.0	0.6
DSD	0.125	0.125	0.25	0.5	0.5
DPM	0.25	0.25	0.5	1.0	2.0

For all DPS observations, both FLUX and INTN grids have been produced. For DSD and DPM observations, only the INTN grid has been produced.

Observations with the following macros are not included with the present data release:

Table 3.2 -- Grid Parameters

Macro	In-scan pixel (')				Cross-scan pixel (')
	12 um	25 um	60mu	100 um	
DNS	0.25	0.25	0.5	1.0	1.0
DPP	0.25	0.25	0.5	1.0	1.0
DPP55D	0.033	0.033	0.066	0.132	0.60
DMS	0.25	0.25	0.5	1.0	1.0

V. PHOTOMETRY ISSUES

i) OVERALL CALIBRATION

The AO grids have been calibrated to the same absolute scale as the IRAS Point Source Catalog. This calibration is based on observations of standard stars and selected asteriods. Details of the absolute calibration can be found in Chapter VI of the Supplement. Flux densities are given in units of Janskys and surface brightnesses are given in units of Janskys/sr at wavelengths of 12, 25, 60, and 100 um assuming the continuum flux density is proportional to frequency to the -1 power. Color correction tables for other energy distributions are given later in this section.

There are a number of systematic errors, typically <5%, which depend on the flux of the source, the background, and the macro used. The correction factors that should remove these errors are discussed in this section.

ii) FLUX GRID CALIBRATION

The non-linear correction terms are given in Table 4.The effects which are accounted for in this table are:

a) Non-linear load resistor curves -- On the basis of survey results, a three piece fit to the load resistor is apparently more appropriate than the two piece curve originally used in SDAS processing. The difference is mainly important for bright sources or sources observed in high backgrounds.

b) Background dependent frequency response -- In general the response of the detectors speeds up at higher background levels resulting in a background dependent responsivity which is also potentially a function of frequency or scan speed. The shape of the curve is very uncertain, especially at 60 and 100 um. At survey scan speed, we now think there is no variation in the response to point sources with source strength although a variation in response with source strength was incorporated in the SDAS processing. There is evidence (see The Supplement) that at the scan speeds used for the pointed observations, the curve of responsivities versus source strength should also be flat, and a flat curve at the scan speeds of the AOs is assumed in Table 4.

Table 4 -- AO Correction Factors

4.1 -- 12 um

Source Flux Density (Jy)	Background Surface Brightness 14.3	380	3800
	(MJy sr^{-1}) Correction Factor		
1.0	.98	1.00	1.00
2.0	.98	1.00	1.00
3.1	.98	1.00	1.00
4.1	.98	1.00	1.00
5.1	.98	1.00	1.00
6.1	.98	1.00	1.00
7.2	.98	1.00	1.00
8.2	.98	1.00	1.00
9.2	.98	1.00	1.00
10	.98	1.00	1.00
20	1.00	1.00	1.00
31	1.00	1.00	1.00
41	1.00	1.00	1.00
51	1.01	1.00	1.00
61	1.01	1.00	1.00
72	1.02	1.00	1.00
82	1.02	1.00	1.00
92	1.02	1.00	.99
100	1.02	1.00	.99
200	1.02	.99	.99
310	1.02	.99	.98
410	1.02	.99	.97
510	1.01	.98	.97
610	1.01	.96	.96
720	.98	.94	.96
820	.97	.93	.96
920	.95	.91	.96
1000	.94	.91	.96
1500	.91	.88	.96
2000	.90	.88	.97
2600	.90	.88	.97
3100	.91	.88	.97
3600	.91	.89	.97
4100	.91	.89	.98
4600	.91	.89	.98
5100	.91	.89	.98

VERSION 85 OCT 28

Table 4.2 -- 25 um

Source Flux Density (Jy)	Background Surface Brightness 28	220	2200
	(MJy sr^{-1}) Correction Factor		
0.7	.99	1.00	1.01
1.3	.99	1.00	1.01
2.0	.99	1.00	1.01
2.7	.99	1.00	1.01
3.4	.99	1.00	1.01
4.0	.99	1.00	1.01
4.7	.99	1.00	1.01
5.4	.99	1.00	1.01
6.0	.99	1.00	1.01
6.7	.99	1.00	1.01
13	.99	1.00	1.01
20	.99	1.00	1.01
27	1.00	1.00	1.01
34	1.01	1.00	1.00
40	1.01	1.00	1.00
47	1.01	1.00	1.00
54	1.00	1.00	1.00
60	1.00	1.00	1.00
67	1.00	1.00	1.00
130	1.00	1.00	.99
200	1.01	1.00	.99
270	1.01	1.01	.98
340	1.01	1.00	.97
400	1.00	.98	.97
470	.98	.97	.97
540	.97	.96	.97
600	.96	.95	.97
670	.95	.94	.97
1000	.92	.91	.97
1300	.92	.92	.98
1700	.92	.92	.98
2000	.92	.92	.98
2300	.93	.92	.98
2700	.93	.92	.99
3000	.93	.93	.99
3400	.93	.93	.99

VERSION 85 OCT 28

Table 4.3 -- 60 um

Source Flux Density (Jy)	Background Surface Brightness 5.9	198	1980
	(MJy sr^{-1}) Correction Factor		
1.3	1.03	1.01	1.00
3	1.04	1.01	1.00
4	1.04	1.01	1.00
5	1.04	1.01	1.00
6	1.04	1.01	1.00
8	1.04	1.01	1.00
9	1.04	1.01	1.00
10	1.04	1.01	1.00
12	1.04	1.01	1.00
13	1.04	1.01	1.00
26	1.02	1.01	1.00
38	1.01	1.00	1.00
51	1.01	1.00	1.00
64	1.00	1.00	1.00
77	1.00	1.00	1.00
90	.99	1.00	1.00
100	.99	1.00	1.00
115	.99	1.00	1.00
130	.99	1.00	1.00
260	.98	1.00	.99
380	.98	1.00	.98
510	.98	1.00	.98
640	.98	1.00	.97
770	.98	1.00	.96
900	.98	1.00	.96
1000	.98	1.00	.95
1150	.97	.98	.95
1300	.96	.98	.95
1900	.93	.94	.93
2600	.90	.92	.93
3200	.89	.91	.93
3800	.89	.91	.94
4500	.89	.92	.94
5100	.90	.92	.94
5800	.90	.92	.94
6400	.90	.92	.94

VERSION 85 OCT 28

Table 4.4 -- 100 um

Source Flux Density (Jy)	Background Surface Brightness 8.29	286	2860
	(MJy sr^{-1}) Correction Factor		
4.2	1.04	1.00	1.00
8.3	1.04	1.00	1.00
12.5	1.03	1.00	1.00
16.7	1.03	1.00	1.00
21	1.03	1.00	1.00
25	1.02	1.00	1.00
29	1.02	1.00	1.00
33	1.02	1.00	1.00
38	1.02	1.00	1.00
41	1.02	1.00	1.00
83	1.00	1.00	1.00
125	.99	1.00	1.00
167	.99	1.00	1.00
209	.98	1.00	1.00
250	.98	.99	1.00
292	.98	.99	1.00
334	.97	.99	1.00
375	.97	.99	1.00
417	.97	.99	1.00
834	.95	.99	.99
1250	.95	.99	.98
1670	.96	.99	.97
2080	.96	.99	.97
2500	.96	.99	.96
2920	.96	.99	.96
3340	.96	1.00	.95
3750	.96	1.00	.95
4170	.96	.99	.94
6260	.93	.96	.93
8340	.91	.94	.91
10400	.89	.92	.91

VERSION 85 OCT 28

Macro Dependent Corrections

The correction factors used in producing the grids are the average values for the DPS macros in the FLUX mode. There are also macro dependent corrections which are listed in Table 5. They have been determined using a series of observations of NGC6543 with the various macros. These factors reflect the small differences which come about because the gains in the flux mode filtering were not precisely known at the start of processing. Table 5 is taken from the April 22, 1985 memo "MACRO and Cross-scan Dependent Calibration Correction Factors for Pass 2 DPS Macros (FLUX mode)" by E.L.Kopan (IOM 85-SDAS-109).

Strictly speaking, the calibration correction factors apply only to the prime track of the macro. For the DPS macros, the prime track went through detector 37 (see The Supplement), and was the track taken by the targeted source in the observation. Variations of up to 10% have been observed for other tracks in the focal plane. These focal plane variations are being mapped and will be incorporated in an IPAC source extractor.

Table 5 -AO Macro Dependent Corrections*

	correction factors/sigma				
Macro	12 um	25 um	60 um	100 um	N obs
DPS(average)	1.000/.04	1.000/.03	1.000/.05	1.000/.05	108
DPS02B	1.004/.03	0.992/.03	1.010/.04	1.020/.04	14
DPS60B	1.018/.04	0.996/.04	0.965/.02	1.041/.04	15
DPS60C	1.015/.04	1.003/.04	0.990/.03	1.060/.03	10
DPS60D	0.980/.02	0.988/.03	1.014/.04	0.930/.03	16
DPS61C	1.047/.03	1.026/.02	1.000/.01	1.065/.01	7
DPS61D	0.994/.03	0.997/.02	1.032/.05	0.992/.03	14
DPS62D	0.999/.03	1.020/.03	1.024/.03	1.005/.05	4
DPS63D	0.987/.04	1.006/.02	0.982/.03	0.991/.04	14
DPS52B	0.990/.03	1.001/.03	1.001/.08	0.967/.02	14

* This factor is the ratio of the flux density of NGC6543 as determined in the IRAS final absolute calibration to that derived by processing NGC6543 with the macro in question.

Color Corrections

The instrumental fluxes have been converted into flux densities at the wavelengths of 12, 25, 60 and 100 um assuming that the true shape of the input continuum distribution is constant in the flux per logarithmic frequency interval, i.e., if the flux density goes as the frequency nu to the minus one power. For energy distributions other than nu^{-1}, a color correction needs to be applied. Table 6 gives the color corrections K for a range of blackbody temperatures and for a number of power law energy distributions. The corrections are applied using the formula:

Flux Density[actual] = Flux Density[quoted]/K

A more complete discussion of color corrections can be found in the Supplement, Section VI-C.3.

Table 6 -- Color Correction Factors K

	Blackbody					Power Law			
Temp(K)	Effective Wavelength				Index	Effective Wavelength			
	12	25	60	100		12	25	60	100
10000	1.45	1.41	1.32	1.09	-3.0	0.91	0.89	1.02	1.02
5000	1.43	1.40	1.32	1.09	-2.5	0.92	0.91	1.00	1.01
4000	1.42	1.40	1.31	1.09	-2.0	0.94	0.93	0.99	1.00
3000	1.41	1.39	1.31	1.09	-1.5	0.97	0.96	0.99	1.00
2000	1.38	1.38	1.31	1.09	-1.0	1.00	1.00	1.00	1.00
1000	1.27	1.34	1.29	1.08	-0.5	1.04	1.04	1.02	1.00
800	1.22	1.32	1.28	1.08	0.0	1.10	1.10	1.05	1.01
600	1.15	1.29	1.27	1.08	0.5	1.17	1.16	1.09	1.02
500	1.09	1.26	1.26	1.08	1.0	1.25	1.23	1.15	1.04
400	1.01	1.22	1.24	1.08	1.5	1.35	1.32	1.23	1.06
300	0.92	1.15	1.21	1.07	2.0	1.47	1.41	1.32	1.09
280	0.90	1.14	1.20	1.07	2.5	1.61	1.53	1.44	1.12
260	0.88	1.12	1.19	1.07	3.0	1.78	1.67	1.59	1.16
240	0.86	1.09	1.18	1.07					
220	0.85	1.07	1.17	1.07					
200	0.83	1.04	1.16	1.06					
180	0.83	1.01	1.14	1.06					
160	0.84	0.97	1.12	1.06					
140	0.87	0.93	1.09	1.05					
120	0.94	0.89	1.06	1.04					
100	1.12	0.84	1.02	1.04					
90	1.28	0.83	1.00	1.03					
80	1.54	0.81	0.97	1.02					
70	2.01	0.81	0.95	1.01					
60	2.97	0.83	0.93	1.00					
50	5.35	0.90	0.91	0.99					
40	13.79	1.08	0.93	0.98					

Coadding errors

When coadding grids using the IPAC coadding program DSGAD, the sampling and positional uncertainties introduce an effective decrease on the response of order 10%. The best values deduced so far are that the fluxes from coadded grids must be increased by factors of:

12 um	1.09
25 um	1.08
60 um	1.07
100 um	1.05.

The effect appears not to be cumulative after the first coaddition.

Example

As an example of the use of the FLUX correction factors, consider a 12 um source detected in a DPS61D observation which has the following characteristics:

Flux density = 32.3 Jy	[from FLUX obs]
Background level = 14.3 M Jy sr^{-1}	[from INTN obs or FITS header]

From the table of non-linear correction terms we find that the correction factor for this background and source flux density is 1.00. The corrected flux density is thus 32.3 * 1.00 Jy. This would correspond to the value listed in the Catalog of IRAS Point Sources.

Since the observation was made using a DPS61D macro, the macro correction factor of 0.994 should be applied to the flux density. The fully corrected flux is then,

Flux Density = 32.3 * 0.994
= 32.1 Jy

Finally, if the continuum were determined to vary as a 1000 K blackbody, the true flux density would be (from Table 6)

flux density (1000K) = 32.1 /1.27 Jy
= 25.3 Jy.

As can be seen from this example, all corrections except the color correction are very close to unity and can generally be ignored.

FLUX Grid Uncertainties

The processes associated with producing the final AO product are so varied and dependent on the actual conditions of the observation, that it is impossible to estimate the systematic uncertainties for a general case. It is necessary to discuss various contributions separately. The following discussion concerns the photometric accuracy of point sources extracted from flux mode grids.

The absolute calibration in the sense of a knowledge of the flux densities of a set of stars and asteroids has an estimated uncertainty of 2, 5, 5 and 10 percent in the 12, 25, 60 and 100 um bands, respectively (see the Supplement).

The IRAS array sensitivity is dependent on the cross-scan position of the source. The current uncertainty in the cross-scan responsivity relative to the prime track results in an uncertainty which is less than 10 percent.

If the assumptions about the frequency dependent responsivity and the non-linearity of the load resistor are correct, the uncertainties introduced by the corrections of Table 4 are less than 3 %. This is expected to be the case for all the sources at 12 and 25 um and for 25 and 60 um sources fainter than NGC6543. The discussion in the Supplement indicates that for the brightest sources the responsivity may vary with frequency by a factor of 60%. Although most of the sources looked at with the AOs are much fainter than those for which variations have been demonstrated, some residual non-linearities are almost certainly present

The pointed observations are calibrated via flashes of an internal reference source; see the Supplement. When scans were made near the Galactic plane or in other highly crowded regions where the backgrounds are high, the flashes are frequently so confused that they are rejected by the calibration processor, and the calibration transfer is from a distant reference source flash. Approximately 20% of all the AO's (primarily in the molecular cloud and galactic structure programs) are effected by this rejected reference flash problem. For the 12, 25, and 60 um bands the responsivities of the detectors were constant to better than +/- 12% (See Figure IV.A.2 of the Supplement), so the worst case error would be ~24%. For the 100 um band the dispersion in detector responsivities was about twice that of the other bands.

The coadding of various grids has very non-Gaussian uncertainties. Although the uncertainties in the correction factor are generally statistically less than 5 percent, grids with large position errors can introduce large uncertainties and errors of 40 percent have been seen because of this effect. The user is advised to inspect the component grids before performing a coadd. Not only can instrumental problems be identified, but asteroids and variable sources can be found.

The repeatability of flux estimates is generally measured to be in the range 5 - 10 percent. It depends on the binning of the sources in the extraction and on the alignment and reproducability of the scan tracks.

For FLUX grids, nearby sources can cause errors in both flux and in position of weaker sources. The error is due to the presence of negative lobes in the filter response of the point source filter and extends to roughly one source width beyond the usual half power point.

In summary, under normal conditions the uncertainties in the results of coadded FLUX mode AOs are generally of order 15 percent. The uncertainties are, however, so non-Gaussian that each case must be looked at and understood individually in the context of the specific measurement.

iii) INTENSITY GRID CALIBRATION

The INTENSITY grids, like the FLUX mode observations, have been nominally corrected to the IRAS absolute calibration scale used for the Point Source Catalog. It is assumed that no macro-dependent calibration factors are needed for very extended sources. The non-linear corrections are less than 5%.

The POINT SOURCE photometric accuracy of the INTENSITY mode observations has been investigated by comparing integrated fluxes from INTENSITY grids with fluxes derived from FLUX mode grids. In general, the INTENSITY fluxes agree well with the FLUX mode values. However, for certain cross scan positions, there are errors of up to 50% or more. These errors are due to the extreme undersampling of the focal plane in cross scan due to dead or noisy detectors. The greatest dispersions are associated with detector 25 in the 12 um band, detectors 42,17, and 20 in the 25 um band, and detector 36 in the 60 um band. The noise weighting can also contribute photometric dispersion of order 10-20%. The cross scan response has been modeled for sources larger than point source angular size. As expected, the dispersion due to undersampling decreases as the source angular diameter increases. For a 5' small extended source, the INTENSITY mode cross scan response is uniform to the 10 percent level. Based on this study we make the following recommendations:

1. INTENSITY grids should NOT be used to obtain point source fluxes unless the user is willing to accept the large uncertainties involved.
2. INTENSITY grids should provide useful integrated fluxes for sources greater than ~5' in diameter.

To facilitate the display of the grids, an average baseline equal to the 25th percentile value of all the pixels has been subtracted from the data. This baseline value appears in the FITS header under the non-standard keyword "BIAS" and has units of Jy/Sr. Due to an error in the IRAS calibration software, the BIAS value does not properly reflect the absolute intensity above zero but differs by an additive number that depends on the particulars of the observation. We estimate the error to be under 30% near the ecliptic poles where the background is lowest, and less for regions of higher background. For absolute intensities, the Zodiacal History File values can be consulted for points nearby in position, time, and solar elongation. The proper baseline corrections have been applied to that data set.

VI. ANALYSIS OF POINTED OBSERVATION QUALITY

The bulk of the pointed observation quality analysis used the Additional Observation Job (AOJ) source extraction file at IPAC. The AOJ is a quick look product that includes contour plots and source extractions for all the AOs processed at IPAC. By using the source extractor outputs of the FLUX grids, positional and photometric repeatability of virtually all the grids could be checked. Since matching FLUX and INTENSITY grids are derived from the same data, the positional accuracy of one version is shared by the other.

i) The AOJ Source Extractor

The AOJ source extractor uses a simple thresholding algorithm. Two thresholds, a MEDIAN signal to noise ratio and a LOCAL signal to noise ratio must be passed for a candidate source to be consdered for further analysis. The MEDIAN NOISE is an estimate of the standard deviation of the coadded pixel values in the entire grid. It is a reasonable approximation to the general noise level for uncomplicated fields and an overestimate for fields with many sources. (See Section V.C of the Supplement for a discussion of median noise estimators.) The source extractor identifies pixels with a flux greater than 3.0 times the median noise of the grid, and adjacent candidate pixels are then combined into single sources. An additional threshold is used to eliminate "sources" due to radiation hits and other spurious events. The LOCAL NOISE is an estimate of the standard deviation of the samples going into a given pixel. These values comprise the NOISE map that accompanies each band SIGNAL map. The method used to calculate the LOCAL NOISE is described in Section IV of this document. For the analysis that follows, we consider only sources with a peak SIGNAL/LOCAL NOISE greater than 4.5.

ii) Pointing

Repeatability of the pointing was investigated by comparing source extractions from grids with overlapping sky coverage. A 60" by 150" window around each source was searched for candidate matches. Figures 3a-3h are histograms of the in-scan and cross- scan distances from the refined position of the source. The refined position is an average position from the two grids, hence, a corresponding histogram of the position differences between sources in the two grids would have a horizontal scale 1.4 times larger. The histograms for the four bands indicate a high repeatability from observation to observation. The grid to matching grid comparison forms the basis for the quality checking algorithm as described in Section VII.

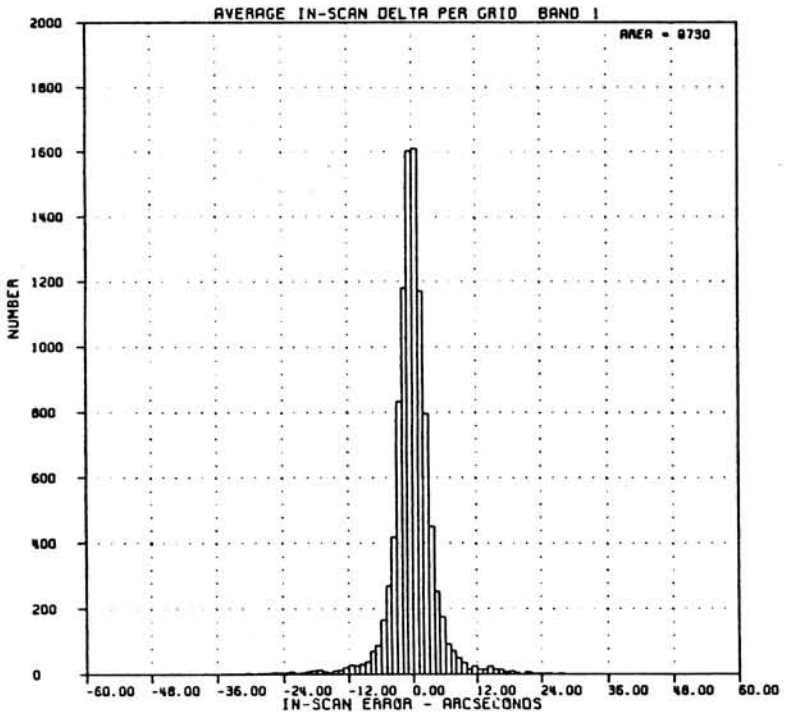

Figure 3a. Average In-Scan Error Histogram for 12 um Band.

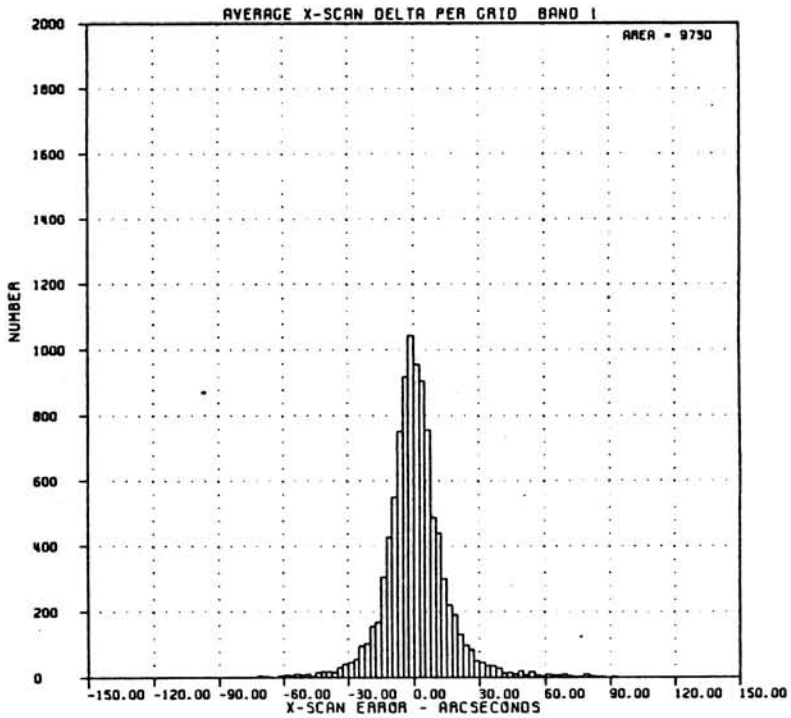

Figure 3b. Average Cross-Scan Error Histogram for 12 um Band.

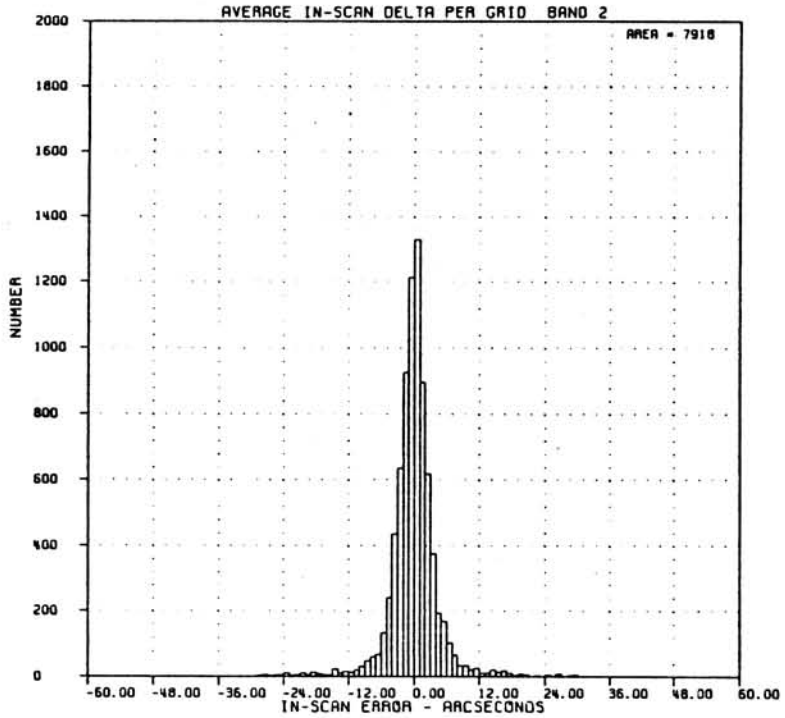

Figure 3c. Average In-Scan Error Histogram for 25 um Band.

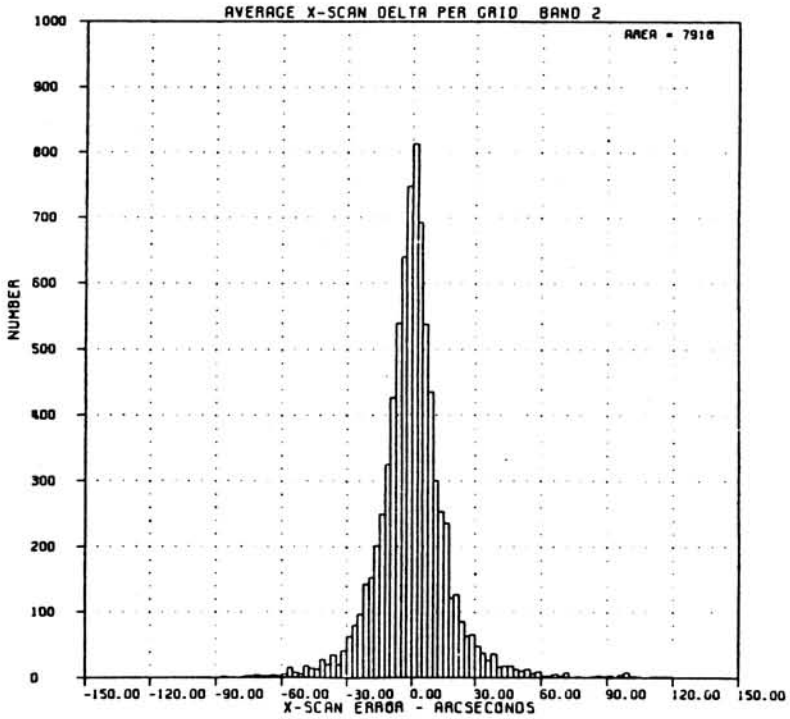

Figure 3d. Average Cross-Scan Error Histogram for 25 um Band.

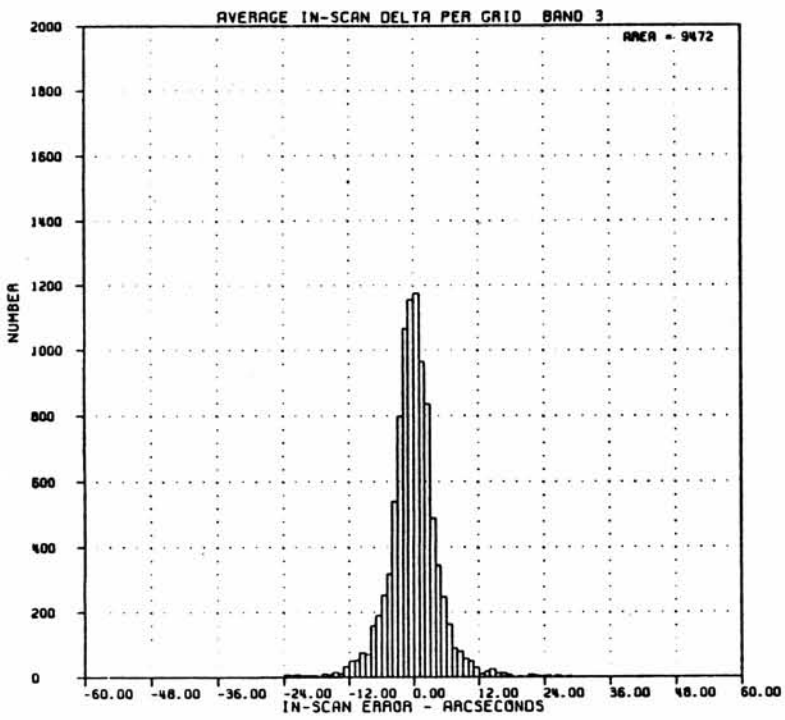

Figure 3e. Average In-Scan Error Histogram for 60 um Band.

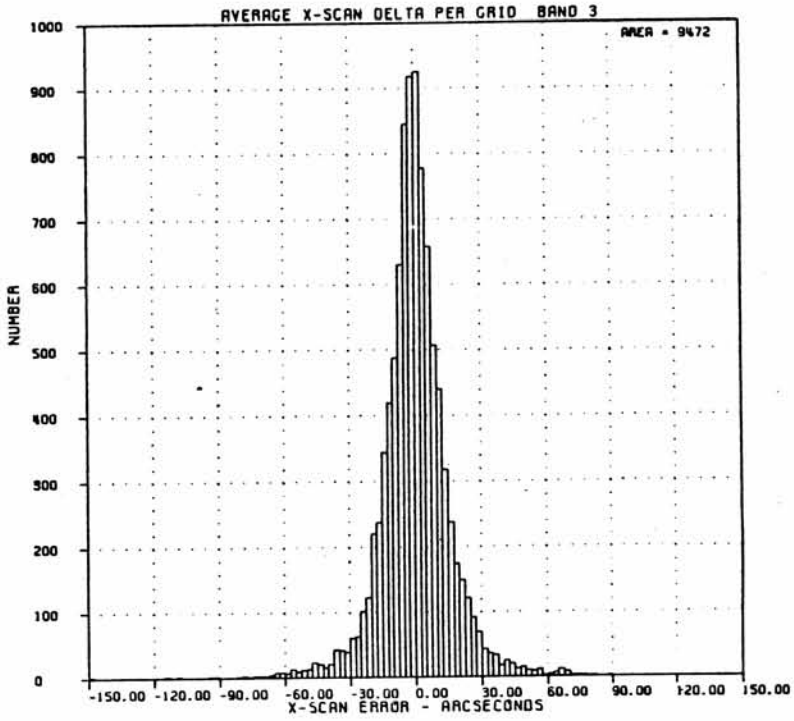

Figure 3f. Average Cross-Scan Error Histogram for 60 um Band.

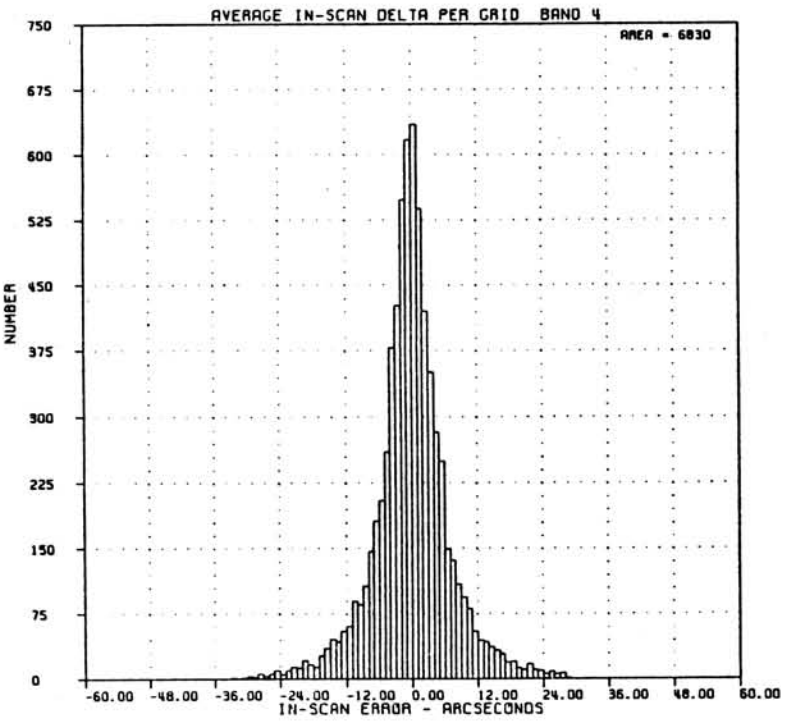

Figure 3g. Average In-Scan Error Histogram for 100 um Band.

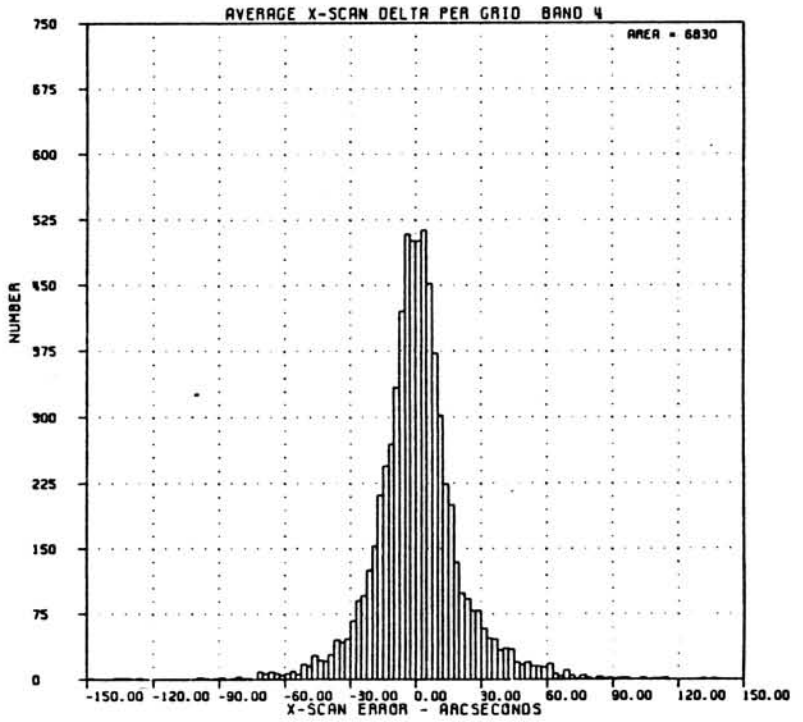

Figure 3h. Average Cross-Scan Error Histogram for 100 um Band.

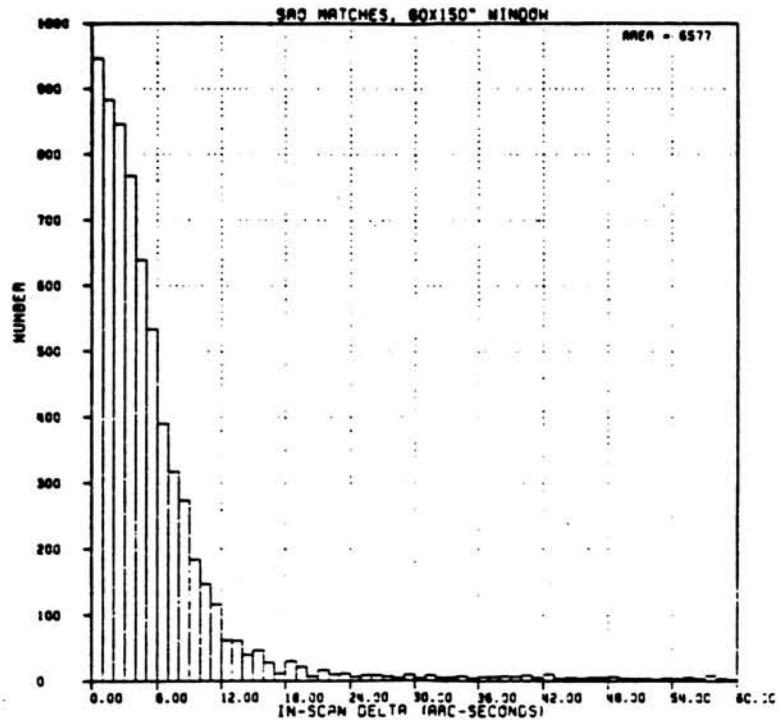

Figure 4a. In-Scan Error Histogram for SAO Stars

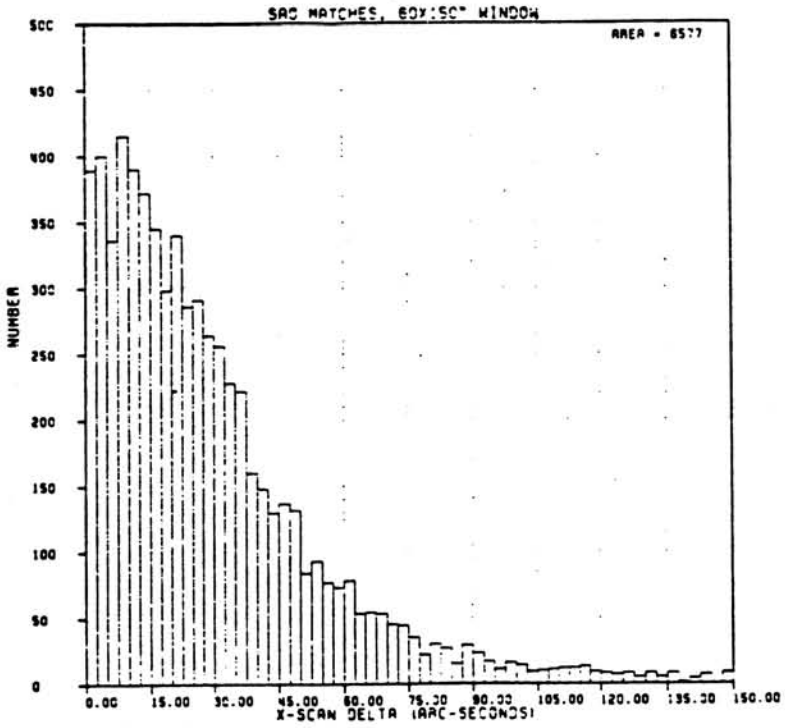

Figure 4b. Cross-Scan Error Histogram for SAO Stars.

To investigate the absolute pointing accuracy of the AOs, positions for all extracted 12 um sources were compared to positions of stars in the SAO Catalog. A box 60" in-scan and 150" cross scan around the extracted position was searched, and 6577 matches were made. Figures 4a and b show histograms of the absolute differences between the catalog and AO positions. The in-scan distribution is closely Gaussian with a sigma of ~7". The low level tail to the distribution is consistent with chance associations. The cross-scan distribution has a sigma of ~35".

iii) Photometry

A series of calibration stars were observed using primarily the DPS macros. The flux densities for these stars were compared to the values for the same stars found in the Point Source Catalog. The various non-linear corrections described in Section IV have been applied to the data. Table 7 gives the magnitude differences for these stars. No systematic trends as a function of source strength are evident, although there appear to be small differences in the mean scales. For the wide range of flux densities, the two data products are consistent. It is important to note that the signal to noise ratios of the stellar observations at 100 um are quite low, and the absolute calibration described in Section V of this document is more reliable. The absolute calibration of the IRAS Point Source Catalog is discussed in Chapter VI of the Supplement.

Table 7. Comparison of AO Photometry with IRAS Point Source Catalog for Standard Stars

	12um		25um		60um		100um	
STAR	PSC	PSC-AO	PSC	PSC-AO	PSC	PSC-AO	PSC	PSC-AO
α Aur	-1.90	-0.03	-1.95	-0.04	-1.85	+0.16	-1.85	+0.11
α CMa	-1.35	-0.03	-1.39	-0.05	-1.23	+0.12	-1.74	+0.11
α CMi	-0.71	+0.01	-0.73	-0.04	-0.72	+0.09	----	---
β Gem	-1.21	-0.04	-1.19	-0.04	-1.22	+0.04	-1.19	+0.14
α Leo	+1.58	-0.18	+1.62	-0.12	---	---	---	---
α UMa	+1.99	-0.15	+1.92	-0.16	---	---	---	---
α Boo	-3.22	-0.15	-3.09	-0.01	-3.02	+0.10	-3.02	+0.19
α Lyr	-0.02	-0.06	-0.17	+0.03	-1.94	+0.10	-3.00	+0.15
β Gru	-3.40	-0.07	-3.50	-0.05	-3.52	0.00	-3.51	+0.19

iv) Additional Quality Issues

A number of additional points should be kept in mind when using the pointed observations.

a) Full Depth Coverage Region in the Map

The depth of coverage in the maps produced with the DPS and DPM macros is not uniform. This non-uniformity arises because the detectors for a given band are grouped into two segments (see the Supplement, p. II-11). For example, the 12 um band consists of two detector segments separated by approximately 15'. Since the maps present data for the entire region covered by the detectors, there are regions at both ends of the map covered by detectors of just a single segement. With only half the integration time, the sensitivity for the single coverage region is roughly 1.4 times worse than the central region of the map.

Since the DSD macro used the output of a single detector per band, the coverage is uniform for those observations.

b) Noisy Tracks in the Maps

Several of the detectors were subject to low level noise pick-up from the 1 Hz spacecraft clock. Since the rastering motion for the macros was also tied to this clock, there were cases where the noise sychronously coadded during the observation. The most prominent example of this effect is in the 12 um band with the DPS52B macro. For many of those observations, a line of sources at cross scan position Z ~ 12, and every 1.93' in-scan (every 1 second of time at the 1.93'/sec scan rate) can be seen. At the single observation level, the vast majority of the false sources have a local signal to noise ratio worse than 4.5, and can be rejected on that basis. If maps with these pulses are coadded, however, the signal to noise ratio will often improve as would be the case for genuine sources.

Macros that incorporated a cross scan step (such as DPS02B and DPS62D) tend not to have this problem. The rastering period was not an exact multiple of 1 second, and the clock pick-up did not sychronously coadd during the observation.

c) Saturated Pixels

Of the 13853 grids delivered in this release, 294 were made of very bright objects where the on-board analog to digital converter (ADC) saturated at the gain used. These saturated observations are identified in Appendix D on a band by band basis. Usually, only a few pixels in the map are saturated, with the rest being usable. In some of the cases, the observations were repeated at lower gain, and the user should consult the Directory for all the observations of a given region.

VII. SELECTION OF GRIDS FOR RELEASE

The overall strategy of verifying the quality of the pointed observations for release rests on using repeated observations of the same region of the sky. During the mission, the observations were scheduled using the guideline that all objects were to be observed at least twice. Confirmation of sources is particularly important in using the IRAS data since many asteroids were detected. Of 14656 grids (both FLUX and INTN) with acceptable macros, 708 did not have an overlapping observation. Under the guidelines for the data release of November 1985, these grids are not included in the present distribution.

i)Guiding Principles

In selecting observations for release five basic principles were applied:

1. Only grids of macro-types DPS, DPM or DSD should be released.

2. Only grids with another, confirming grid of the same macro-type covering essentially the same piece of sky should be released,

3. Only grids with proveably bad pointing should be withheld, the primary quality problem with the grids being poor pointing.

4. Only a crude flux consistency test was required, and

5. If an INTENSITY grid had a corresponding FLUX grid, only the FLUX grid needed to be checked for positional accuracy.

ii) Grid Selection

For each of the three main macro classifications grid selection took place in three steps. The first step in the process was checking the grids for confirming partners. This check demanded that the center of one grid lie less than five arcminutes away from another grid of the same macro-type. Grids satisfying this criterion moved on to the next stage of selection.

For the next step all grids were organized into time-ordered "stacks", the component grids of which covered one field on the sky and thus mutually confirmed. The grids in these confirming stacks were then intercompared in pairs to attempt to verify consistent pointing.

Sources from each grid in each band were selected to be compared, seeking matches in order to confirm good pointing or prove bad pointing. In each grid, only sources away from the grid borders, lying on the comparing grid and with a local signal to noise ratio of 3.5 or more

were allowed to compare. Two sources were considered a match if they were within 30 arc-seconds in-scan and 75 arc-seconds cross-scan of one another. For the DPS grids only, the extracted fluxes were required to be within a factor of two of one another. If a source had multiple matches, only the best match was kept.

Once a match was found the positions of the two matched sources were combined to produce a single refined position to which both component sources were then compared. The in-scan and cross-scan distances from each source to the refined position were averaged with similar determinations from all other matches in all bands to produce an estimate of the pointing error between the two grids.

Before the average in-scan and cross-scan errors for a given grid pair were accepted there had to be: (1) at least two matches among all the bands or (2) one match where the matching sources had LOCAL signal to noise ratios of 10 or greater and flux agreement to within 30%.

If one grid of the pair had a significant pointing error with respect to the other, the error would show up in one of two ways: (1) the average pointing error was more than 15 arcseconds in-scan or 30 arcseconds cross-scan, or (2) no matches among the two grids was found despite the existence of valid candidates for matching on both grids.

If a grid failed this intercomparison check with all other grids in the stack it was declared to have bad pointing. Note that the grids in a stack of two grids obviously had only one chance at intercomparison. If one of the grids was bad, both grids failed because the grid with bad pointing will be withheld, leaving the other grid without a confirming partner.

If a pair of grids did not have any candidate extractions of sufficient signal to noise ratio for matching between them, and therefore no matches, the grid pair was still passed, based on the very low rejection rate of verifiable grids.

The steps outlined above to check for confirming grids and to verify good pointing accuracy for each grid were automated. The program produced a list of grids which appeared to fail the release criteria. Because of the complexity of the observing program and the infrared sky, as well as the imperfections of programmers, the contour plots from the quick-look output for the rejected grids were examined by hand to confirm the conclusions of the automatic checker.

The hand analysis of the rejected grids allowed a number of these grids to pass. First, 109 observations from the SY (Solar System) and CM (Comet) programs failed the grid pair criterion. Since these were observations of moving objects, a suitable grid pair was unlikely. We have chosen to pass all these observations, but the user is cautioned to independently verify the quality of the pointing. Second, 133 grids had no or only very faint candidate sources for confirmation. No reliable verification of the pointing was possible for these grids. Again, we have chosen to pass these grids as not proven faulty. The justification for this pass philosophy is based on the very low failure rate for the grids that can be checked. Of these 242 unverified grids, we expect no

more than one grid with bad pointing. Finally, 18 DSD observations were passed based on inspection of the contour plots. In these cases, the source extractor output gave erroneous results due to the very complicated nature of the targeted fields.

iii) Results

Table 8 summarizes the results of the pointing verification process. Roughly 0.6% of the grids have been rejected due to bad pointing.

Table 8. Summary of Quality Checking

Grids with acceptable macros	14656
Grids passed by automatic process	13605
Grids failed by automatic process	1051
Restored by hand analysis:	
SY or CM observations	109
No sources for matching	133
Complicated field but acceptable	18
Total restored by hand analysis	260
Rejected Grids:	
Grids with no paired grid	708
Grids with bad pointing	89
Grids with processing problems	6
Total Failed	803
Total Number of Grids Delivered	13853

APPENDIX A. FORMAT OF THE IRAS POINTED OBSERVATIONS

This section describes the formats of the Additional Observation (AO) Directory and AO Grids in their machine readable forms. The AOs were produced on a set of 66 volumes of 9-track, 6250 bpi, unlabeled tapes. The order of the AOs on the tapes reflects various mission and post-mission constraints. In general, the data are ordered on the tapes according to time of observation. The directory, which is ordered according to increasing Right Ascension of the grid center, is the key to finding the desired AO. The tape volumes are numbered in the form IRGnmm, where n is a data center code and mm is the volume number between 01 and 66.

I. The AO Directory

The AO Directory is the key to locating an IRAS pointed Observation on the tapes. The directory is ordered according to increasing Right Ascension of the grid center. It is available in printed form as Appendix C of this document and as a machine-readable file on the tape volume (IRG100). The machine-readable AO Directory is the first file on Tape IRG101. Physical record size is 2880 bytes. Each logical record is 120 bytes long and describes one AO grid. Bytes are numbered 0 to 119, and each contains on 7-bit, right justified ASCII character. The format for each of the logical records is given in Table A.1

Each observation consists of eight files on the tape: 12 um data, 12 um noise, 25 um data, 25 um noise, 60 um data, 60 um noise, 100 um data, and 100 um noise. For brevity, the file number for only the 12 um data grid is listed in the directory. The file numbers for the other bands and the noise grids can computed by adding the appropriate offset to the 12 um number.

Table A.1 FORMAT OF THE AO DIRECTORY

START BYTE	NAME	DESCRIPTION	UNITS	FORMAT
0	RA	Right Ascension (1950) of grid	degrees	F9.4
9	DEC	Declination (1950) of grid	degrees	F9.4
18	ROTA	Rotation angle (FITS CROTA2) from +Y Axis to +DEC	degrees	F8.2
26	Y	Y-axis (in-scan) grid dimension	arcmin	I4
30	Z	Z-axis (cross-scan) grid dimension	arcmin	I4
34	---	SPACE	-----	1X
35	MACRO	Macro of this observation.	-----	A6
41	---	SPACE	-----	1X
42	OBSID	Observation identifier	-----	A6

Table A.1 FORMAT OF THE AO DIRECTORY continued

START BYTE	NAME	DESCRIPTION	UNITS	FORMAT
48	GRID	Grid number.	-----	I6
54	----	SPACE	-----	1X
55	MODE	Mode of processing. F= FLUX grid I= INTN grid	-----	A2
57	OBSDAT	Observation date, day of month	-----	I2
59	----	"/"	-----	A1
60	OBSDAT	Observation date, month	-----	I2
62	----	"/"	-----	A1
63	OBSDAT	observation date, year	-----	I2
65	----	SPACE	-----	A1
66	VOL	Tape volume for this grid, e.g., IRGmnn where : m is a data-center designator code delivered to: 1 NSSDC 2 RAL, UK 3 U. Leiden, Netherlands 9 IPAC nn is the tape volume number	-	A6
72	FILE	File number for the 12 um data grid Note: File N+1 contains the 12 um noise File N+2 contains the 25 um data File N+3 contains the 25 um noise File N+4 contains the 60 um data File N+5 contains the 60 um noise File N+6 contains the 100 um data File N+7 contains the 100 um data	-	I5
77	BITS	Bits per data pixel (16 or 32)	-	I3
80	B1NOISE	Per band median noise for this grid. Units are Jy for FLUX grids and Jy/Sr for INTENSITY grids.	Jy[/Sr]	E9.2
89	B2NOISE		Jy[/Sr]	E9.2
98	B3NOISE		Jy[/Sr]	E9.2
107	B4NOISE		Jy[/Sr]	E9.2
116	SPARE	All ASCII zeros	-	4A1

2. The AO Grids

The magnetic tape form of the Additional Observations contains the coadded grid data arrays of pixels recorded in the FITS format. The article by Wells, Greisen, and Harten [Astron. and Astrophys. Suppl., 44, 363-370 (1981)] in conjunction with the header record for each grid give a detailed description of the format of each grid.

Each observation is represented by eight files on the tape: 12 um data, 12 um noise, 25 um data, 25 um noise, 60 um data, 60 um noise, 100 um data, and 100 um noise. The first two records of each file contain the FITS header, then the grid begins in the third record as a stream of pixel values divided into 2880 byte records without regard to line length. The final records is padded to 2880 bytes with zeros. Two-byte integers are used for most of the FLUX and INTN data grids and all of the noise grids. In a few cases, four-byte integers are used to avoid saturation.

Standard FITS keywords are used where possible. Explanations and nonstandard keywords are given in Table A.2.

Table A.2 FITS KEYWORDS

KEYWORD	EXPLANATION
BZERO	BZERO is meant to define the photometric baseline. This parameter is set to zero for all the IRAS grids. For INTN grids, a baseline equal to the 25th percentile of the intensity values in the grid has been subtracted to produce the values on the tape. This baseline value is given under the non-standard keyword BIAS.
BUNIT	The FLUX data and noise grids are in Jy. The INTN grids have units of Jy/Sr.
CDELT1	This parameter is negative since increasing samples along axis 1 are in the -RA direction.
CROTA2	This angle defines the rotation from the +Y axis (in-scan) toward the +DEC axis, where counter-clockwise angles are positive.
BIAS	This nonstandard keyword gives the estimated baseline for INTN grids. It corresponds to the 25th percentile of the intensity values in the grid. The true brightness in a pixel is given by: TRUE = TAPE * BSCALE + BIAS For FLUX grids, the BIAS level is given for reference only. The true flux level in the pixel is given by: TRUE = TAPE * BSCALE

Table A.2 FITS KEYWORDS continued

KEYWORD	EXPLANATION
DATE-OBS	The UT date of the observation.
DATE	The PST date that the FITS format version of this grid was processed.
DSKYGRID	A nonstandard keyword. DSKYGRID gives the identification number of the grid assigned during the initial processing at SDAS.
DATE-CR	A nonstandard keyword. DATE-CR is the date of the initial processing at SDAS.
OBJECT	Identifies the scientific program and sequence number for this observation. In general, repeated observations of the same position in the sky will have the same OBJECT designation.
OBSERVER	Identifies the macro used for the observation. Macro characteristics are given in Table 2 of this guide.

Table A-3. SAMPLE FLUX GRID HEADER

```
SIMPLE  =                    T  /STANDARD FITS FORMAT
BITPIX  =                   16  /2 BYTE TWOS-COMPL INTEGERS
NAXIS   =                    3  /NUMBER OF AXES
NAXIS1  =                   50  /NZ = Z (CROSS SCAN) GRID DIMENSION
NAXIS2  =                  216  /NY = Y (IN SCAN) GRID DIMENSION
NAXIS3  =                    1  /NUMBER OF WAVELENGTHS
BSCALE  =       1.611655E-02    /TRUE=TAPE*BSCALE+BZERO
BZERO   =       0.0
BUNIT   = 'JY     '             /FLUX
BLANK   =                -32768 /TAPE VALUE FOR EMPTY CELL
CRVAL1  =       8.282030E+02    /RA AT ORIGIN (DEGREES)
CRPIX1  =                 26.   /Z-AXIS ORIGIN (CELL) = (NZ/2)+1
CTYPE1  = 'RA---SIN'            /DECREASES IN VALUE AS SAMPLE INDEX
COMMENT                          INCREASES (ORTHOGRAPHIC PROJECTION)
CDELT1  =       9.999998E-02    /Z-GRID CELL WIDTH (DEGREES)
CROTA1  =                0.0    /TWIST ANGLE UNDEFINED FOR Z-AXIS
CRVAL2  =       2.206647E+01    /DEC AT ORIGIN (DEGREES)
CRPIX2  =                109.   /Y-AXIS ORIGIN (CELL) = (NY/2)+1
CTYPE2  = 'DEC--SIN'            /INCREASES IN VALUE AS LINE INDEX
COMMENT                          INCREASES (ORTHOGRAPHIC PROJECTION)
CDELT2  =       8.333333E-03    /Y-GRID CELL WIDTH (DEGREES)
CROTA2  =       2.750000E+01    /ROTATES +NAXIS2 INTO +DEC AXIS (ANGLE
COMMENT                          MEASURED POSITIVE CCW FROM +NAXIS2 TO
COMMENT                          +DEC)   (DEGREES)
CRVAL3  =           6.00E-05    /WAVELENGTH IN METERS
CRPIX3  =                 1.
CTYPE3  = 'LAMBDA'
CDELT3  =                 0.
CROTA3  =                 0.
DATAMAX =       4.612556E+00    /JY      (TRUE VALUE)
DATAMIN =      -2.651172E-01    /JY      (TRUE VALUE)
BIAS    =       2.728472E+07    /BIAS LEVEL (GRID REF) IN JY/SR
EPOCH   =               1950.   /EME50
DATE-OBS = '15/ 3/83'           /DATE OF OBSERVATION (DD/MM/YY)
DATE    = '15/10/85'            /DATE THIS TAPE WRITTEN (DD/MM/YY)
ORIGIN  = 'JPL-IRAS'            /INSTITUTION
TELESCOP = 'IRAS    '
INSTRUME = 'DEEPSKY '
COMMENT                          DSSID = DS01
COMMENT                          SOP =    98; OBS =    13
DSKYGRID =                838.  /DEEPSKY GRID NO.
DATE-CR  = '41442254'           /DSCO O/P FILE CREATION DATE(YDDDHHMM)
COMMENT                         EST. MEDIAN NOISE =3.1673E-02 JY
COMMENT                         GRID TWIST =-1.7725000E+02 (DEG) MEAS-
COMMENT                         URED FROM SOUTH TO +Y, CW IS POSITIVE.
COMMENT                         GAIN NORM. USED = 1.590000E-01
COMMENT                         MFILT = 6
COMMENT                         KFILT = 6
OBJECT  = 'BS   64'             /OBSERVER ID + IGO'S AO NO.
COMMENT                          IGO'S REP. SEQ. NO. = 2
OBSERVER = 'DPS52B '            /DS01,2 SIS: C1 FIELD
COMMENT                         OBJ. NAME NO. (C2) FIELD =1
COMMENT                         DS01,2 SIS: D(1-4) = 5 31 42  0
COMMENT                         DS01,2 SIS: E(1-3) =111 59 29
COMMENT                         DS01,2 SIS: PROG = DPS1AB
COMMENT   REFERENCES:
COMMENT   IRAS SDAS SOFTWARE INTERFACE SPEC. #623-94/NO. DS01
COMMENT   IRAS SDAS SOFTWARE INTERFACE SPEC. #623-94/NO. DS02
COMMENT   THE USER'S GUIDE TO IRAS POINTED OBSERVATION PRODUCTS
COMMENT   IRAS/SDAS SUBSYSTEM DESIGN SPEC./ #623-75
COMMENT   ASTRON. ASTROPHYS SUPPL SER. 44, 363-370 (1981)
```

Table A-4. SAMPLE INTENSITY GRID HEADER

```
SIMPLE  =                    T  /STANDARD FITS FORMAT
BITPIX  =                   16  /2 BYTE TWOS-COMPL INTEGERS
NAXIS   =                    3  /NUMBER OF AXES
NAXIS1  =                   50  /NZ = Z (CROSS SCAN) GRID DIMENSION
NAXIS2  =                  216  /NY = Y (IN SCAN) GRID DIMENSION
NAXIS3  =                    1  /NUMBER OF WAVELENGTHS
BSCALE  =       3.528288E+04    /TRUE=TAPE*BSCALE+BZERO
BZERO   =       0.0
BUNIT   =  'JY/SR  '            /INTN
BLANK   =              -32768   /TAPE VALUE FOR EMPTY CELL
CRVAL1  =       8.282030E+02    /RA AT ORIGIN (DEGREES)
CRPIX1  =                 26.   /Z-AXIS ORIGIN (CELL) = (NZ/2)+1
CTYPE1  =  'RA---SIN'           /DECREASES IN VALUE AS SAMPLE INDEX
COMMENT                          INCREASES (ORTHOGRAPHIC PROJECTION)
CDELT1  =       9.999998E-02    /Z-GRID CELL WIDTH (DEGREES)
CROTA1  =       0.0             /TWIST ANGLE UNDEFINED FOR Z-AXIS
CRVAL2  =       2.206647E+01    /DEC AT ORIGIN (DEGREES)
CRPIX2  =                109.   /Y-AXIS ORIGIN (CELL) = (NY/2)+1
CTYPE2  =  'DEC--SIN'           /INCREASES IN VALUE AS LINE INDEX
COMMENT                          INCREASES (ORTHOGRAPHIC PROJECTION)
CDELT2  =       8.333333E-03    /Y-GRID CELL WIDTH (DEGREES)
CROTA2  =       2.750000E+01    /ROTATES +NAXIS2 INTO +DEC AXIS (ANGLE
COMMENT                          MEASURED POSITIVE CCW FROM +NAXIS2 TO
COMMENT                          +DEC)   (DEGREES)
CRVAL3  =           6.00E-05    /WAVELENGTH IN METERS
CRPIX3  =                 1.
CTYPE3  =  'LAMBDA'
CDELT3  =                 0.
CROTA3  =                 0.
DATAMAX =       1.040139E+08    /JY/SR   (TRUE VALUE)
DATAMIN =      -9.879207E-01    /JY/SR   (TRUE VALUE)
BIAS    =       2.728472E+07    /BIAS LEVEL (GRID REF) IN JY/SR
EPOCH   =               1950.   /EME50
DATE-OBS = '15/ 3/83'           /DATE OF OBSERVATION (DD/MM/YY)
DATE    = '15/10/85'            /DATE THIS TAPE WRITTEN (DD/MM/YY)
ORIGIN  = 'JPL-IRAS'            /INSTITUTION
TELESCOP = 'IRAS    '
INSTRUME = 'DEEPSKY '
COMMENT                          DSSID = DS01
COMMENT                          SOP =    98; OBS =    13
DSKYGRID =              839.    /DEEPSKY GRID NO.
DATE-CR  =  '41442254'          /DSCO O/P FILE CREATION DATE(YDDDHHMM)
COMMENT                         EST. MEDIAN NOISE =3.1673E-02 JY
COMMENT                         GRID TWIST =-1.7725000E+02 (DEG) MEAS-
COMMENT                         URED FROM SOUTH TO +Y, CW IS POSITIVE.
COMMENT                         GAIN NORM. USED = 8.600000E-01
COMMENT                         MFILT = 1
COMMENT                         KFILT = 0
OBJECT  = 'BS   64'             /OBSERVER ID + IGO'S AO NO.
COMMENT                          IGO'S REP. SEQ. NO. = 2
OBSERVER = 'DPS52B '            /DS01,2 SIS: C1 FIELD
COMMENT                         OBJ. NAME NO. (C2) FIELD =1
COMMENT                         DS01,2 SIS: D(1-4) = 5 31 42  0
COMMENT                         DS01,2 SIS: E(1-3) =111 59 29
COMMENT                         DS01,2 SIS: PROG = IPS1AB
COMMENT    REFERENCES:
COMMENT    IRAS SDAS SOFTWARE INTERFACE SPEC. #623-94/NO. DS01
COMMENT    IRAS SDAS SOFTWARE INTERFACE SPEC. #623-94/NO. DS02
COMMENT    THE USER'S GUIDE TO IRAS POINTED OBSERVATION PRODUCTS
COMMENT    IRAS/SDAS SUBSYSTEM DESIGN SPEC./ #623-75
COMMENT    ASTRON. ASTROPHYS SUPPL SER. 44, 363-370 (1981)
```

Table A-5. SAMPLE NOISE GRID HEADER

```
SIMPLE  =                    T  /STANDARD FITS FORMAT
BITPIX  =                   16  /2 BYTE TWOS-COMPL INTEGERS
NAXIS   =                    3  /NUMBER OF AXES
NAXIS1  =                   50  /NZ = Z (CROSS SCAN) GRID DIMENSION
NAXIS2  =                  216  /NY = Y (IN SCAN) GRID DIMENSION
NAXIS3  =                    1  /NUMBER OF WAVELENGTHS
BSCALE  =       1.611655E-02    /TRUE=TAPE*BSCALE+BZERO
BZERO   =       0.0
BUNIT   =  'JY      '           /NOIS (STATISTICAL WEIGHT)
BLANK   =               -32768  /TAPE VALUE FOR EMPTY CELL
CRVAL1  =       8.282030E+02    /RA AT ORIGIN (DEGREES)
CRPIX1  =                 26.   /Z-AXIS ORIGIN (CELL) = (NZ/2)+1
CTYPE1  =  'RA---SIN'           /DECREASES IN VALUE AS SAMPLE INDEX
COMMENT                          INCREASES (ORTHOGRAPHIC PROJECTION)
CDELT1  =       9.999998E-02    /Z-GRID CELL WIDTH (DEGREES)
CROTA1  =                0.0    /TWIST ANGLE UNDEFINED FOR Z-AXIS
CRVAL2  =       2.206647E+01    /DEC AT ORIGIN (DEGREES)
CRPIX2  =                109.   /Y-AXIS ORIGIN (CELL) = (NY/2)+1
CTYPE2  =  'DEC--SIN'           /INCREASES IN VALUE AS LINE INDEX
COMMENT                          INCREASES (ORTHOGRAPHIC PROJECTION)
CDELT2  =       8.333333E-03    /Y-GRID CELL WIDTH (DEGREES)
CROTA2  =       2.750000E+01    /ROTATES +NAXIS2 INTO +DEC AXIS (ANGLE
COMMENT                          MEASURED POSITIVE CCW FROM +NAXIS2 TO
COMMENT                          +DEC)   (DEGREES)
CRVAL3  =           6.00E-05    /WAVELENGTH IN METERS
CRPIX3  =                 1.
CTYPE3  =  'LAMBDA'
CDELT3  =                 0.
CROTA3  =                 0.
DATAMAX =       4.448168E+00    /JY      (TRUE VALUE)
DATAMIN =       1.611655E-02    /JY      (TRUE VALUE)
EPOCH   =               1950.   /EME50
DATE-OBS = '15/ 3/83'           /DATE OF OBSERVATION (DD/MM/YY)
DATE    = '15/10/85'            /DATE THIS TAPE WRITTEN (DD/MM/YY)
ORIGIN  = 'JPL-IRAS'            /INSTITUTION
TELESCOP = 'IRAS    '
INSTRUME = 'DEEPSKY '
COMMENT                          DSSID = DS01
COMMENT                          SOP =    98; OBS =    13
DSKYGRID =              838.    /DEEPSKY GRID NO.
DATE-CR  =  '41442254'          /DSCO O/P FILE CREATION DATE(YDDDHHMM)
COMMENT                         EST. MEDIAN NOISE =3.1673E-02 JY
COMMENT                         GRID TWIST =-1.7725000E+02 (DEG) MEAS-
COMMENT                         URED FROM SOUTH TO +Y, CW IS POSITIVE.
COMMENT                         GAIN NORM. USED = 1.590000E-01
COMMENT                         MFILT = 6
COMMENT                         KFILT = 6
OBJECT   = 'BS - 64'            /OBSERVER ID + IGO'S AO NO.
COMMENT                          IGO'S REP. SEQ. NO. = 2
OBSERVER = 'DPS52B '            /DS01,2 SIS: C1 FIELD
COMMENT                         OBJ. NAME NO. (C2) FIELD =1
COMMENT                         DS01,2 SIS: D(1-4) = 5 31 42  0
COMMENT                         DS01,2 SIS: E(1-3) =111 59 29
COMMENT                         DS01,2 SIS: PROG = DPS1AB
COMMENT    REFERENCES:
COMMENT    IRAS SDAS SOFTWARE INTERFACE SPEC. #623-94/NO. DS01
COMMENT    IRAS SDAS SOFTWARE INTERFACE SPEC. #623-94/NO. DS02
COMMENT    THE USER'S GUIDE TO IRAS POINTED OBSERVATION PRODUCTS
COMMENT    IRAS/SDAS SUBSYSTEM DESIGN SPEC./ #623-75
COMMENT    ASTRON. ASTROPHYS SUPPL SER. 44, 363-370 (1981)
```

APPENDIX B. FORTRAN Subroutines to Convert Between RA-DEC and Pixel Coordinates

These three FORTRAN subroutines can be used to convert between equatorial coordinates and the pixel coordinates of the IRAS pointed observations. The grids have been produced using an orthographic projection. Epoch 1950 has been assumed throughout the processing. Subroutine CTE2G computes the transformation matrix used by the other subroutines and needs to be run only once per grid. The subroutines GTOSKY and SKYTOG compute the grid to sky and sky to grid conversions, respectively.

```
C *****COMPUTE EME50 TO GRID TRANSFORMATION MATRIX********
C
      SUBROUTINE CTE2G(ALPG,DELG,CROTA2,TE2G)
C
C     TE2G   =  TRANSFORMATION MATRIX FROM EME TO GRID
C     ALPG   =  RIGHT ASCENSION OF GRID CENTER (DEG, EME50)
C     DELG   =  DECLINATION OF GRID CENTER (DEG, EME50)
C     CROTA2 = GRID ROTATION ANGLE.  IN FITS HEADER.
C
      REAL*8 TE2G(3,3)
      DATA RTD/57.29577951/
C
      TWSG = CROTA2 - 180.0
      SALP = SIN(ALPG/RTD)
      CALP = COS(ALPG/RTD)
      SDEL = SIN(DELG/RTD)
      CDEL = COS(DELG/RTD)
      STWS = SIN(TWSG/RTD)
      CTWS = COS(TWSG/RTD)
C
      TE2G(1,1) = +SDEL
      TE2G(1,2) = -SALP*CDEL
      TE2G(1,3) = +CALP*CDEL
      TE2G(2,1) = -CDEL*CTWS
      TE2G(2,2) = -CALP*STWS -SALP*SDEL*CTWS
      TE2G(2,3) = -SALP*STWS +CALP*SDEL*CTWS
      TE2G(3,1) = +CDEL*STWS
      TE2G(3,2) = -CALP*CTWS +SALP*SDEL*STWS
      TE2G(3,3) = -SALP*CTWS -CALP*SDEL*STWS
C
      RETURN
      END
```

```
C     *****CONVERT PIXEL (PY,PZ) TO RA AND DEC (ALP,DEL)****
C
        SUBROUTINE GTOSKY(PY,PZ,NY,NZ,DRY,DRZ,TE2G,ALP,DEL)
C
C       PY   =  Y (IN-SCAN) PIXEL VALUE
C       PZ   =  Z (CROSS-SCAN) PIXEL VALUE
C       NY   =  NUMBER OF CELLS IN Y DIRECTION
C       NZ   =  NUMBER OF CELLS IN Z DIRECTION
C       DRY  =  CELL SIZE IN Y DIRECTION (ARCMINUTES)
C       DRZ  =  CELL SIZE IN Z DIRECTION (ARCMINUTES)
C       TE2G =  TRANSFORMATION MATRIX FROM EME TO GRID
C               COMPUTED IN SUBROUTINE CTE2G
C       ALP  =  RIGHT ASCENSION OF PIXEL PY,PZ (DEG, EME50)
C       DEL  =  DECLINATION OF PIXEL PY,PZ  (DEG, EME50)
C
        INTEGER*4    NY,NZ,NYC,NZC
        REAL*4       ALPG,DELG,TWSG,ALP,DEL,PY,PZ
        REAL*8       TE2G(3,3), VE(3), VT(3)
        DATA         RTD /57.29577951/
C
C       COMPUTE GRID VECTOR
C
        NYC = NY/2 + 1
        NZC = NZ/2 + 1
        VT(2) = (PY - NYC) * DRY / (60. * RTD)
        VT(3) = (PZ - NZC) * DRZ / (60. * RTD)
        VT2   = 1. - VT(2) * VT(2) - VT(3) * VT(3)
        VT(1) = SQRT( VT2 )
C
C       COMPUTE EME VECTOR AND RA, DEC
C
        VE(1) = TE2G(1,1)*VT(1)+TE2G(2,1)*VT(2)+TE2G(3,1)*VT(3)
        VE(2) = TE2G(1,2)*VT(1)+TE2G(2,2)*VT(2)+TE2G(3,2)*VT(3)
        VE(3) = TE2G(1,3)*VT(1)+TE2G(2,3)*VT(2)+TE2G(3,3)*VT(3)
        CDEL  = VE(2)*VE(2) +VE(3)*VE(3)
        CDEL  = SQRT(CDEL)
        SDEL  = VE(1)
        DEL   = RTD * ATAN2( SDEL, CDEL)
        SALP  = -VE(2)
        CALP  =  VE(3)
        ALP   = RTD * ATAN2( SALP, CALP )
        IF ( ALP .LT. 0. ) ALP = ALP + 360.
C
        RETURN
        END
```

```
C  *********CONVERT RA & DEC (ALP,DEL) TO PIXEL (PY,PZ)********
C
      SUBROUTINE SKYTOG(PY,PZ,NY,NZ,DRY,DRZ,TE2G,ALP,DEL)
C
C     PY   =  Y (IN-SCAN) PIXEL VALUE
C     PZ   =  Z (CROSS-SCAN) PIXEL VALUE
C     NY   =  NUMBER OF CELLS IN Y DIRECTION
C     NZ   =  NUMBER OF CELLS IN Z DIRECTION
C     DRY  =  CELL SIZE IN Y DIRECTION (ARCMINUTES)
C     DRZ  =  CELL SIZE IN Z DIRECTION (ARCMINUTES)
C     TE2G =  TRANSFORMATION MATRIX FROM EME TO GRID
C             COMPUTED IN SUBROUTINE CTE2G
C     ALP  =  RIGHT ASCENSION OF PIXEL PY,PZ (DEG, EME50)
C     DEL  =  DECLINATION OF PIXEL PY,PZ  (DEG, EME50)
C
      INTEGER*4    NY,NZ,NYC,NZC
      REAL*4       ALPG,DELG,TWSG,ALP,DEL,PY,PZ
      REAL*8       TE2G(3,3), VE(3), VT(3)
      DATA         RTD /57.29577951/
C
C     COMPUTE EME VECTOR
C
      NYC = NY/2 + 1
      NZC = NZ/2 + 1
      SDEL = SIN ( DEL/RTD )
      CDEL = COS ( DEL/RTD )
      SALP = SIN ( ALP/RTD )
      CALP = COS ( ALP/RTD )
      VE(1) = +SDEL
      VE(2) = -SALP * CDEL
      VE(3) = +CALP * CDEL
C
C     COMPUTE GRID VECTOR AND PY,PZ
C
      VT(1) = TE2G(1,1)*VE(1)+TE2G(1,2)*VE(2)+TE2G(1,3)*VE(3)
      VT(2) = TE2G(2,1)*VE(1)+TE2G(2,2)*VE(2)+TE2G(2,3)*VE(3)
      VT(3) = TE2G(3,1)*VE(1)+TE2G(3,2)*VE(2)+TE2G(3,3)*VE(3)
      PY    = 60. * RTD * VT(2) / DRY + NYC
      PZ    = 60. * RTD * VT(3) / DRZ + NZC
C
      RETURN
      END
```

Appendix C. The AO Directory

APPENDIX D. GRIDS WITH ADC SATURATION

A number of pointed observations were made of very bright objects in which the analog to digital converter (ADC) on board the spacecraft saturated. These observations and the effected bands are identified in Table D-1.

TABLE D-1 GRIDS WITH SATURATED DATA

GRID NUMBER FLUX, INTN	BANDS 12	25	60	100	GRID NUMBER FLUX, INTN	BANDS 12	25	60	100
119, 120				X	3272, 3273		X	X	X
153, 154			X	X	3306, 3307			X	X
172, 173			X	X	3373, 3374			X	X
195, 196		X	X	X	3381, 3382			X	
212, 213			X	X	3322, 3523			X	X
277, 278		X	X	X	3528, 3529			X	
365, 366			X	X	3538, 3539			X	X
491, 492			X	X	3752, 3753		X	X	X
495, 496			X	X	3794, 3795		X	X	X
584, 585		X	X	X	3814, 3815			X	X
641, 642		X	X	X	3899, 3900			X	X
689, 690		X	X	X	3916, 3917	X			
766, 767		X	X	X	3927, 3928	X			
823, 824		X	X	X	3993, 3994			X	X
832, 833		X	X	X	4105, 4106	X			
857, 858		X	X	X	4684, 4685			X	
863, 864		X	X	X	4707, 4708			X	
950, 951		X	X	X	5113, 5114			X	
989, 990		X	X	X	5140, 5141			X	
1067, 1068		X	X	X	5144, 5145			X	
1218, 1219			X	X	5170, 5171			X	X
1222, 1223		X	X		5174, 5175		X	X	X
1224, 1225		X	X	X	5184, 5185			X	X
1277, 1278		X	X	X	5229, 5230			X	X
1298, 1299		X	X		5274, 5275			X	X
1316, 1317			X	X	5326, 5327			X	
1358, 1359			X	X	5457, 5458			X	
1493			X	X	5461, 5462			X	X
1547			X	X	5540, 5541		X	X	
2541, 2542				X	5561, 5562			X	X
3038, 3039			X	X	5592, 5593			X	
3078, 3079	X	X			5599, 5600				X
3167, 3168			X	X	5619, 5620			X	X
3193, 3194			X		5638, 5639			X	X
3205, 3206			X	X	5641, 5642		X	X	X
3239, 3240			X	X	5651, 5652			X	X

GRID NUMBER		BANDS			
FLUX,	INTN	12	25	60	100
5695,	5696			X	X
5741,	5742			X	X
5745,	5746			X	X
5778,	5779		X	X	X
5876,	5877			X	X
5903,	5904			X	X
5919,	5920	X	X	X	X
	5930			X	
5945,	5946		X	X	X
	5962			X	
5973,	5974	X	X	X	X
6011,	6012				X
6039,	6040	X	X	X	X
6097,	6098	X	X	X	X
6269,	6270		X	X	X
6278,	6279	X	X	X	
6334,	6335			X	X
6354,	6355	X	X	X	
6619,	6620		X	X	
	6642			X	X
6693,	6694			X	X
	6738			X	X
6840,	6841			X	
6971,	6972			X	X
7000,	7001		X	X	X
	7079			X	X
7082,	7083			X	X
	7120	X	X	X	
7128,	7129		X	X	X
	7152			X	X
	7244			X	X
	7255	X	X	X	
	7256			X	
7274,	7275	X	X	X	X
	7344			X	X
	7390			X	
	7479			X	
	7483			X	
	7573			X	
	7592			X	X
	7641			X	
	7738	X			
	7795	X			
7867,	7868			X	
7877,	7878			X	X
	7931	X	X	X	X
	7946		X	X	X
	8004	X	X	X	X
8162,	8163			X	
	8229		X	X	X
8259,	8260			X	
	8370	X	X	X	X
	8391	X	X	X	X

GRID NUMBER		BANDS			
FLUX,	INTN	12	25	60	100
	8407			X	X
	8410			X	X
	8483			X	X
	8510			X	X
	8535			X	X
8850,	8851			X	X
	8962		X	X	X
8971,	8972			X	X
	8977		X	X	X
	9014			X	X
	9023			X	X
	9077			X	X
	9184		X	X	X
	9310	X			
9745,	9746			X	
9782,	9783			X	X
	10182		X	X	X
10319,	10320			X	X
10541,	10542			X	
10863,	10864		X	X	X
10951,	10952		X	X	X
	11002				X
	11090				X
	11363			X	X
	11735			X	X
	11749			X	X
	11840		X	X	X
11946,	11947			X	
	12127			X	X
	12548				X
	12744			X	X
	12778			X	X
	12887			X	X
	12894				X
	13020	X	X	X	X
	13059	X	X	X	X
13112,	13113				X
13118,	13119			X	
13177,	13178				X
13378,	13379			X	
	13782		X	X	
13951,	13952	X			
	14098		X	X	
	14320		X	X	
14418,	14419	X	X		
	14691			X	
	14709	X	X		
	14827			X	
	14862	X	X		
14922,	14923	X	X		
	14946	X	X		
15358,	15359	X	X		
15442,	15443			X	